Pressure-Induced Phase Separation in Polymer Solutions: Kinetics of Phase Separation and Crossover from Nucleation and Growth to Spinodal Decomposition in Solutions of Polyethylene in *n*-Pentane

Ke Liu and Erdogan Kiran*

Department of Chemical Engineering, Virginia Polytechnic Institute and State University, Blacksburg, Virginia 24061

Received May 11, 2000; Revised Manuscript Received February 12, 2001

ABSTRACT: The kinetics of pressure-induced phase separation (PIPS) in solutions of polyethylene (M_w = 108 000, PDI = 1.32) in *n*-pentane has been studied using time- and angle-resolved light scattering. Controlled pressure quench experiments were conducted at different polymer concentrations (0.49, 0.97, 2.07, 2.8, 4.1, 5.0, and 10.8% by mass) to determine both the binodal and spinodal envelopes and the critical polymer concentration. At each concentration, a series of rapid pressure quenches with different depths of penetration into the region of immiscibility were imposed, and the time evolutions of the scattered light intensities were followed to determine the pressure below which the mechanism changes from "nucleation and growth" to "spinodal decomposition". The crossover is identified from the characteristic fingerprint scattering patterns associated with each mechanism. The spinodal decomposition process is characterized by the formation and evolution of a spinodal ring during phase separation that leads to a maximum in the angular variation of the scattered light intensity. The nucleation and growth mechanism is characterized by the absence of such a maximum and the continual decrease of the scattered light intensities with increasing angles. The time scale of new phase formation and growth is shown to be relatively short. The late stage of phase separation is entered within seconds. For quenches leading to spinodal decomposition, the characteristic wavenumber q_m corresponding to the scattered light intensity maximum I_m is observed to be nonstationary, moving to lower wavenumbers after a very short elapsed time. The growth of domain size is observed to follow power-law-type scaling with $q_m \sim t^{-\alpha}$ and $I_m \sim t^{\beta}$ with $\beta \approx 2\alpha$. In the intermediate and late stages, the domain size is found to grow from 4 to 14 μm within 5 s. Analysis of the early stage of phase separation according to Cahn−Hilliard theory shows that the diffusion coefficients are in the range of (1−9) × 10^{-12} m^2/s and depend on the quench depth.

Introduction

The kinetics of phase separation in polymers is an area of intense research activity. The interest is both theoretical and practical.[1−28] Among the reasons is the desire to understand the time evolution of microstructure development so that practical methodologies can be developed for pinning the nonequilibrium transient structures for specific end uses. The majority of the studies reported in the literature have been on the kinetics of phase separation in "polymer + polymer" blend systems where structure development and morphology control are of great importance.[5,11,21−23] Relatively little work has been done in phase separation kinetics in "polymer + solvent" systems. Studies on "polymer + near-critical or supercritical solvent" systems that form homogeneous solutions at high pressures but phase separate at lower pressures are even more scarce.[12,15,16,18−20] A recent article provides a review of prior work on pressure-induced phase separation in polymer solutions.[12] Polymer processing at high pressures with near-critical and supercritical fluids is however a new growth area, and there is now much interest in understanding the dynamic aspects of miscibility and phase separation. In these systems, pressure-induced phase separation (PIPS) poses new challenges in experimentation and theory and offers new opportunities. A special advantage of PIPS is that pressure can be changed rapidly in the entire bulk of the solution, and the two-phase regions can be entered faster than would be feasible by other common techniques. This is in contrast to temperature-induced or solvent-induced phase separation since uniform and rapid temperature or compositional change in the entire bulk of the solution would not be as easy due to heat and mass transfer limitations.

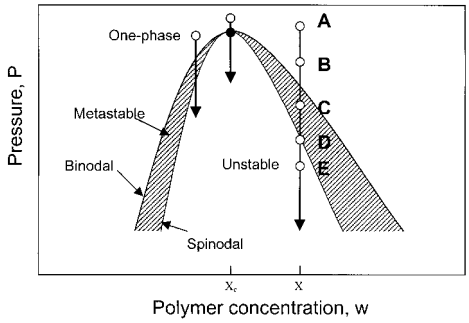

Figure 1. Schematic representation of the pressure-induced phase separation and the pressure quench path to different depths of penetration.

Some of the basic elements associated with polymer solutions at high pressures are demonstrated in Figure 1, which is a pressure−composition diagram at a given temperature. The region above the binodal curve corresponds to the homogeneous one-phase solution condition. The region inside the spinodal envelope represents the thermodynamically unstable region where all concentration fluctuations result in a decrease of free energy and lead to a spontaneous phase separation. In the metastable region between the binodal and the

* Author for correspondence: Tel 540-231-4213, Fax 540-231-5022; E-mail ekiran@vt.edu.

10.1021/ma000816k CCC: $20.00
Published on Web 03/29/2001

spinodal the solution is stable to small fluctuations but undergoes phase separation for large concentration fluctuations. As shown in the figure, by following a path such as A through E, two-phase regions can be entered by lowering the pressure at a given concentration. When metastable regions are entered, phase separation is expected to proceed by the nucleation and growth mechanism. When unstable regions are entered, the mechanism of phase separation is that of spinodal decomposition. It should be clear from the figure that, except at the critical polymer concentration, whether the phase separation should proceed by nucleation and growth or by spinodal decomposition will depend on the depth of penetration (the magnitude of the pressure quench) into the region of immiscibility. These mechanisms are distinguishable from the "fingerprint" characteristics of the angular dependence and time evolution of the scattered light intensities after the imposed quench. By conducting controlled and progressively deeper pressure quenches, the crossover of the phase separation mechanism from nucleation and growth to spinodal decomposition can be documented.

We have recently developed a methodology to experimentally determine the crossover from nucleation and growth to spinodal decomposition using pressure quench and light scattering technique[18,19] which demonstrates the kinetics of phase separation. The technique combines the notion of multiple repetitive pressure drop (MRPD) methodology with time- and angle-resolved light scattering. The experimental system is designed in such a way that at a given polymer concentration the system pressure can be reduced from a point such as A (Figure 1) to a point B or C, and the time evolution of scattered light intensities over a range of angles can be monitored. The solution is then brought back to initial condition A and rehomogenized. Now a second pressure quench is imposed, this time to a lower pressure such as D or E, while again monitoring the time evolution of the scattered light intensities. By carefully selecting the quench depth and observing the light scattering patterns, changes in the phase separation kinetics are noted, and the crossover from metastable to unstable region is identified. The process is repeated for different polymer concentrations, which then permits identification of the width of the metastable region and the experimentally accessible spinodal envolope. With this technique, investigation of the kinetics of spinodal decomposition is not limited to working only at the critical polymer concentration, which is the typical study in temperature-induced phase separation in solutions or in phase separation in polymer−polymer blends. The present technique provides a way to enter the spinodal region at off critical concentrations and permits the documentation of time evolution of phase separation.

Using this technique, we have already reported on the kinetics of pressure-induced phase separation in polystyrene + methylcyclohexane[19,20] and poly(dimethylsiloxane) + supercritical carbon dioxide[18] systems and demonstrated the change in time evolution of the light scattering pattern when phase separation proceeds by nucleation and growth and by spinodal decomposition. For systems undergoing spinodal decomposition, scattered light intensities increase with time and display a scattering maximum in its angular variation that also grows with time. For systems undergoing nucleation and growth, scattered light intensities increase with time without displaying a scattering maximum in its angular dependence.[21−23] A recent article has also reported on the early stage of spinodal decomposition at high pressure in solution of PP in trichlorofluoromethane.[15]

In the present paper, we report on the kinetics of pressure-induced phase separation in solutions of polyethylene in *n*-pentane. To develop the complete information on phase separation of this system, the pressure quench experiments with different penetration depths were conducted at different polymer concentrations. These concentrations were chosen to cover a range below and above the critical polymer concentration.

Experimental Section

Materials. Polyethylene ($M_w = 108\,000$, $M_w/M_n = 1.32$) was obtained from Scientific Polymer Products, and *n*-pentane (purity >99%) was obtained from Aldrich Chemical Corporation and used without further purification.

Light Scattering Apparatus. Figure 2 is the schematic diagram of the multiangle light scattering system used in the pressure quench experiments. Details have been described in earlier publications.[19,20] Briefly, the system is a high-pressure variable-volume light-scattering cell with optical components and fast data acquisition units. A thin stainless steel spacer is used to separate the two flat sapphire windows (SW) and give a short path length of 250 μm. The He−Ne laser beam (λ = 632.8 nm) passes through an iris diaphragm (ID) and a Glen-Thompson polarizer (GTP) and is guided to the center of the scattering cell. On the path of the laser beam after the scattering cell, two convex lenses (L) are placed back-to-back to collect and transfer the scattered light at different angles to a linear image sensor (LIS). A beam splitter (BS) sends the transmitted light to an avalanche photodiode detector (APD). The data acquisition device monitors pressure, temperature, and the transmitted and the scattered light with a computer and a fast data acquisition board. The linear image sensor has 256 pixels that cover an angle range from 1.9° to 12.7°. The data from all angles can be recorded at a rate of 3.2 ms/scan. In a typical experiment, the transmitted light intensities, scattered light intensities at different angles, temperature, and pressure inside the cell are recorded in real time for up to several minutes to document the time evolution of light intensities.

Experimental Procedure. The experiments are conducted by quenching the polymer solutions (PIPS) from the one-phase region to the two-phase region at a given concentration. The pressure quench is achieved by several techniques that are provided with this experimental system. Lowing the pressure of the pressurizing fluid (PF) permits slow pressure reduction through the movement of the movable piston (MP). Turning a dedicated valve (V) can lead to small but rapid pressure quench. Movement of the plunger rod (PR) with air actuation brings about rapid and large pressure quenches. The changes in pressure, temperature, and scattered light intensities are monitored during the phase separation process. During a pressure quench, temperature shows a decrease, the transmitted light decreases, and the scattered light increases. The temperature drop is compensated in a relatively short time because of the heating of the cell. These are schematically shown in Figure 2. The time evolution and the angular variation of the scattered light intensities show different trends if the solution is undergoing phase separation by nucleation and growth (NG) or by spinodal decomposition (SD). These are also shown schematically in Figure 2. The experiments are conducted at each concentration for different quench depths to determine the crossover pressure from one type of phase separation mechanism to another. Systems undergoing spinodal decomposition show a maximum in the angular variation of the scattered light intensities as demonstrated in Figure 2.

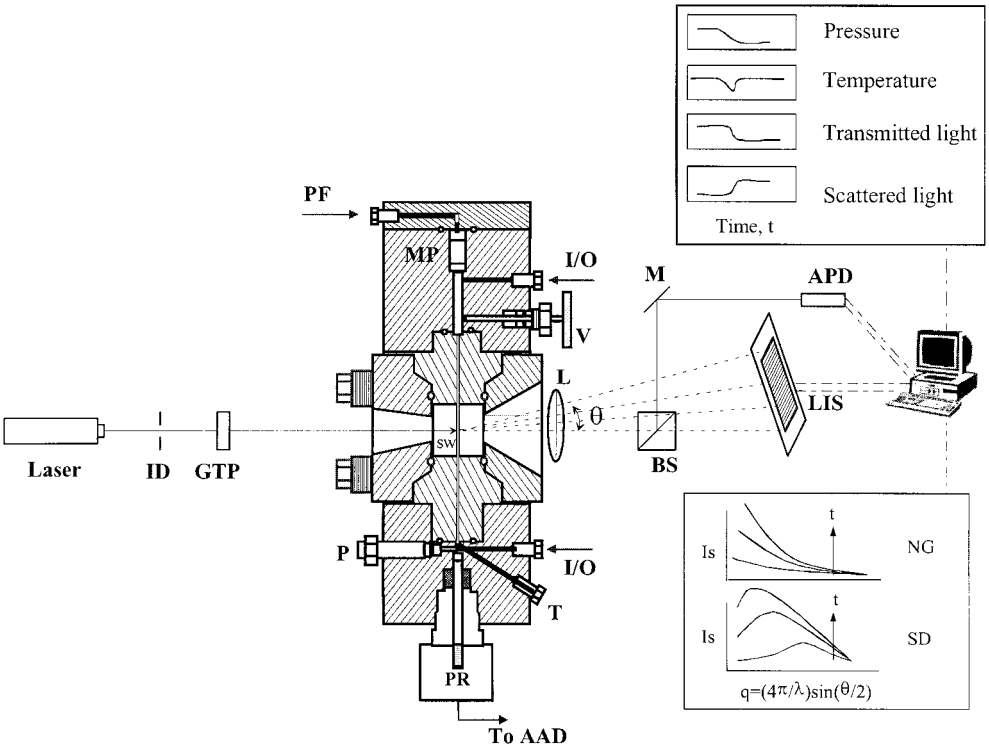

Figure 2. Experimental system: ID = iris diaphragm; GTP = Glan-Thompson polarizer; SW = sapphire window; CL = convex lens; BS = beam splitter; M = mirror; APD = avalanche photodiode detector; LIS = linear image sensor; PR = plunger rod; P = pressure; T = temperature; I/O = inlet and outlet ports; θ = scattering angle; PF = pressurizing fluid; MP = movable piston; I_s = scattering light intensity; NG = nucleation and growth; SD = spinodal decomposition; V = valve.

For systems undergoing phase separation by nucleation and growth mechanism, the angular scattered light intensity does not display such a maximum.

For interpretations of the time evolution of the new phase formation and growth, the scattered light intensities are corrected for turbidity and background scattering.[18−20] The raw data for the scattered light intensity can be corrected first to compensate for the turbidity according to

$$I_{s,corr} = I_{s,raw}/I_{tr,raw} \quad (1)$$

where the scattered light intensity is corrected to the unit basis of the incident light intensity, and $I_{tr,raw}$ and $I_{s,raw}$ are the uncorrected transmitted light and scattered light intensities, respectively. However, this does not account for the presence of background scattering that may arise due to stray lights, internal reflections, or dust that may be present. Therefore, further background subtraction is needed. The following expression is used to obtain the final corrected scattered light intensity $I_{s,\theta,corr(t)}$ at a given scattering angle θ and time t:

$$I_{s,\theta,corr(t)} = [I_{s,\theta(t)}/I_{tr(t)}] - [I_{s,\theta(t=0)}/I_{tr(t=0)}] \quad (2)$$

Here, $I_{tr(t)}$ is the transmitted light intensity and $I_{s,\theta(t)}$ is the raw data for the scattered light intensity. The second term corresponding to time zero is the measure of background scattering in the homogeneous solution prior to the quench. It is this background that is subtracted in obtaining the corrected scattered light intensities.

Results and Discussion

Experiments were conducted at polymer concentrations of 0.49, 0.97, 2.07, 2.8, 4.1, 5.0, and 10.8% by mass. This range was selected to cover concentrations below and above the critical polymer concentration. At each concentration, different quench depths were imposed. Figure 3 shows the results of a slow pressure reduction experiment in 2.07% by mass polymer solution at 423.7 K. The pressure was reduced from about 15.2 MPa to 13.5 MPa over a 40 s period, which corresponds to a pressure quench rate of about 0.04 MPa/s. This is shown in Figure 3B. The temperature remains very stable (Figure 3A) during this slow pressure reduction; only about 0.1 K deviation is observed in this case. The typical cooling effect that is associated with pressure quench is not severe here since the quench speed is relatively slow, which permits the system to be heated back to the initial temperature. The transmitted light intensity (Figure 3C) shows a sudden decrease when the demixing condition is reached. Figure 3B indicates also the variation of inverse scattered light intensities that were averaged for all angle during the quench. This also shows a sudden decrease when a phase boundary is crossed. An alternative method for the assessment of the demixing point is to plot the variation of the inverse scattered light intensity (angle averaged) with pressure, which is shown in Figure 3D. Initially, there is no change in the scattered light intensity above 14 MPa where solution is homogeneous. When the pressure is decreased below 14.0 MPa, the angle-averaged scattered light intensity undergoes a sudden decrease. For this solution, 14.0 MPa is assigned as demixing pressure at 423.7 K.

Figure 4 shows the observation from a more rapid pressure reduction experiment for the same solution at the same initial temperature and pressure. The pressure reduction here is covered from about 14.25 to 13.7 MPa over about 1 s interval corresponding to a quench rate of 0.55 MPa/s, which is about 15 times faster quench speed than the experiment in Figure 3. Here the inverse averaged scattered light intensities vs pressure plots are not as smooth as in the slow pressure reduction case, which does not provide a convenient recording of the demixing pressure. Therefore, in these

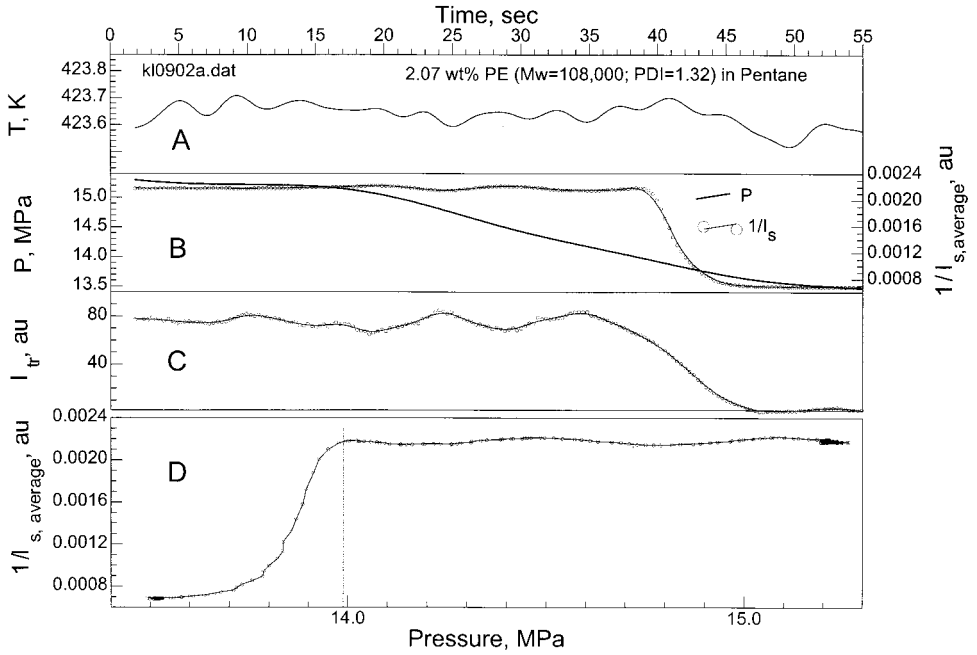

Figure 3. Variation of temperature (T), pressure (P), transmitted light intensity (I_{tr}), and inverse averaged scattered light intensity ($1/I_s$) with time during a slow pressure reduction in 2.07% by mass solution of PE (108K) in *n*-pentane. The demixing pressure is determined from the variation of the inverse scattered light intensity with time or pressure (lower curve in the figure).

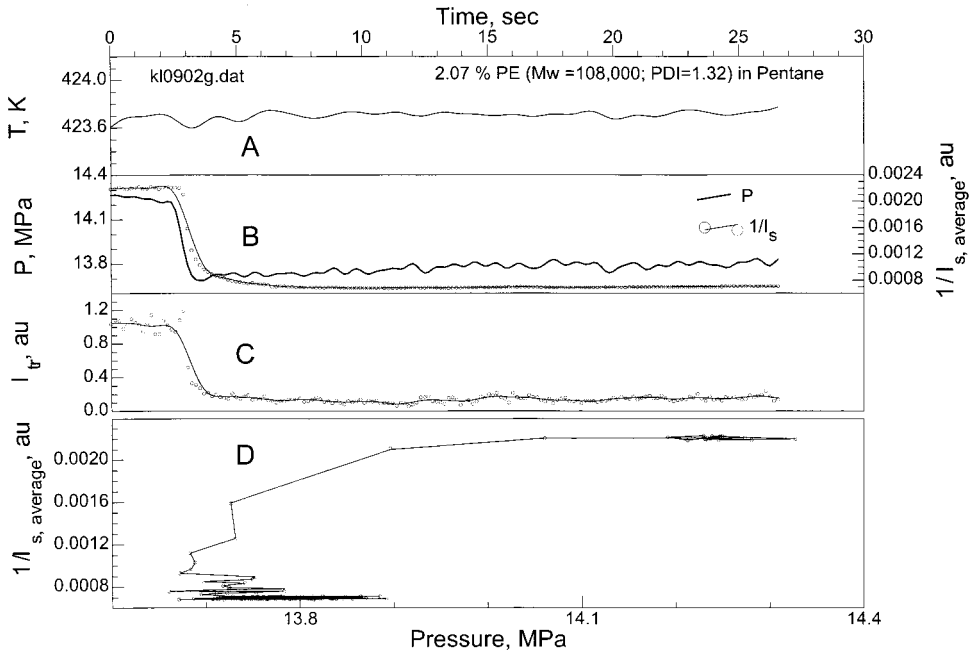

Figure 4. Variation of temperature (T), pressure (P), transmitted light intensity (I_{tr}), and inverse averaged scattered light intensity ($1/I_s$) with time during a fast pressure reduction in 2.07% by mass solution of PE (108K) in *n*-pentane.

cases we analyze the enlarged section of the variation of the I_{tr} or $1/I_{s,average}$ vs time and identify the time corresponding to incipient change in either the transmitted or scattered light intensities. The pressure corresponding to this time is then assumed as the demixing pressure, which in this case was determined to be 14.1 MPa. Even though the difference between the slow and fast quench experiments appears to be small, the dynamic nature of the boundary must be fully recognized. Indeed, as shown in a recent publication in experiments with very rapid quench speed (i.e., in the range 100−400 MPa/s), significant differences in the demixing pressures may be observed.[28] In the assessment of the metastable gap by rapid pressure quench to different depth of penetrations into the region of immiscibility, it is important to first determine the location of the "dynamic" or "apparent binodal boundary". In the present study, to take into account the difference that may arise in the demixing pressure during different quench experiments, at a given concentration at least three different quench experiments with different quench depths were imposed, and the variation was evaluated. The quench depths imposed, even though different, were not very deep. As shown in Table 1, the demixing pressures were close to each other. However, to eliminate ambiguity, the average value of the demixing pressures were taken as the apparent binodal point that is applicable in the quench

Table 1. Binodal and Spinodal Points of Solutions of Polyethylene (M_w = 108 000, PDI = 1.32) in *n*-Pentane T = 423 K

polymer conc, wt %	dynamic demixing press.,[a] MPa			av demixing press., MPa	spinodal press., MPa
	I	II	III		
0.49	12.7 (0.6)	12.7 (0.8)	12.7 (1.6)	12.7	10.6
0.97	12.9 (0.7)	12.9 (0.8)	12.8 (1.5)	12.9	11.8
2.07	14.1 (0.4)	14.1 (0.5)	14.0 (0.9)	14.1	14.1
2.8	13.9 (0.3)	13.9 (0.6)	13.8 (0.8)	13.9	13.8
4.1	13.4 (0.4)	13.4 (1.4)		13.4	13.2
5.0	12.3 (1.0)	12.3 (1.6)	12.2 (3.4)	12.2	9.2
10.8	12.3 (0.8)	12.2 (1.22)	12.2 (2.3)	12.2	NA[b]

[a] The dynamic demixing pressure refers to the demixing pressures obtained during a given pressure quench. The pressure quench depths are indicated in the parentheses after each entry. [b] NA = not accessible up to the maximum pressure quench depth tested, up to ΔP = 2.3 MPa.

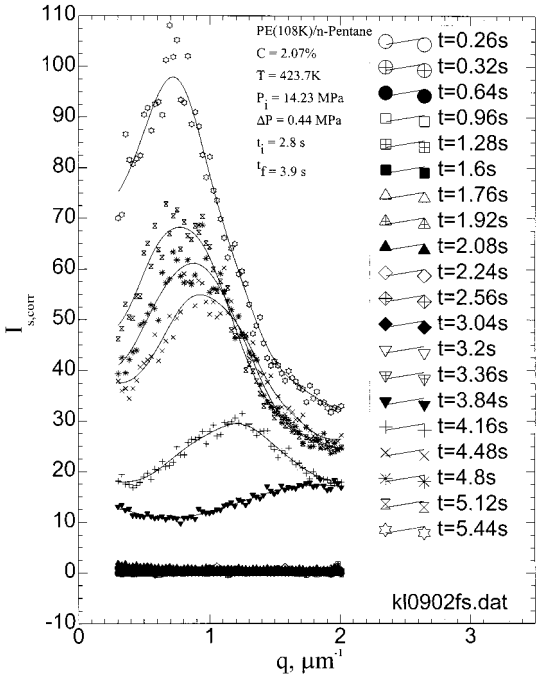

Figure 5. Early part of the evolution of the scattered light intensities with time as a function of the wavenumber q after a pressure quench of ΔP = 0.44 MPa in 2.07% by mass solution of PE (108K) in *n*-pentane at 423.7 K. The total observation time is 5.44 s.

depth intervals imposed. It is realized that the use of the term binodal should be more strictly used in the case of monodisperse polymer systems. As discussed before, the assignment of such an average is important in the assessment of the metastable gap and the spinodal pressure that is determined from such pressure quench experiments.

Figure 5 shows the time evolution of the scattered light intensities as a function of angle (expressed in terms of the wavenumber $q = (4\pi/\lambda)\sin(\theta/2)$) for a quench depth of ΔP = 0.44 MPa for the 2.07% solution. The pressure quench starts at 14.23 MPa, and the final pressure after quench is 13.79 MPa. From Table 1 the demixing pressure assigned at this concentration is 14.1 MPa. The penetration depth into the unstable region from the binodal point in this case is therefore 0.31 MPa. Figure 5 shows a very clear maximum in the variation of the scattered light intensity with angle, which suggests that the system is undergoing spinodal decomposition at this quench depth. The spinodal ring is observable at 3.84 s, which corresponds to 1 s collapse time

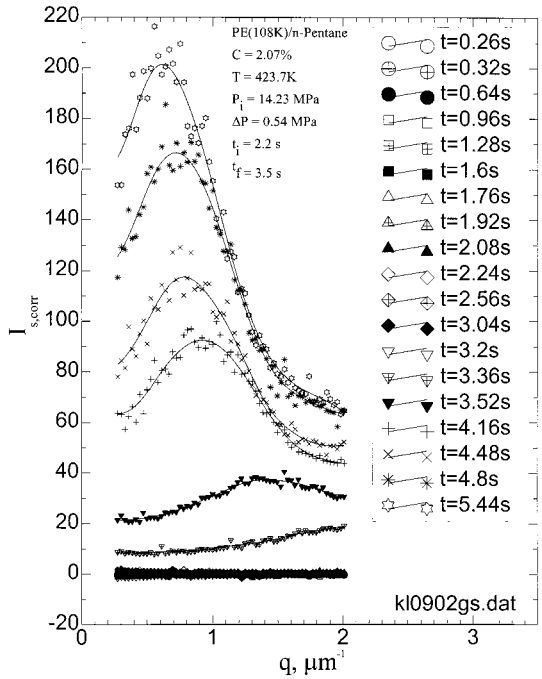

Figure 6. Early part of the evolution of the scattered light intensities with time as a function of the wavenumber q after a pressure quench of ΔP = 0.54 MPa in 2.07% by mass solution of PE (108K) in *n*-pentane at 423.7 K. The total observation time is 5.44 s.

after initiation of the quench and becomes distinct at 4.16 s, which corresponds to about 200 ms after completion of the quench. The angular position of the maximum of the scattered light intensity is however not stationary and moves to lower angles (low q values) with time.

Figure 6 shows the result for a pressure quench of 0.54 MPa. The spinodal ring is distinctly observed at t = 3.52 s, which is shortly after (20 ms) the pressure reaches its minimum. Compared to the 0.44 MPa quench, in this deeper quench experiment, scattered light intensities become more intense, even though not shown in the figure, ring collapse occurs faster (within 8 s for 0.54 MPa quench vs 12 s for 0.44 MPa quench[24]). The spinodal ring observed for this solution for quenches as shallow as 0.1 MPa below the binodal suggests that the concentration (i.e., 2.07%) must be close to the critical polymer concentration.

Figure 7 shows the evolution of the scattered light intensities for the polymer at a lower concentration, at 0.97%, at the same temperature subjected to a relatively deep quench of 1.9 MPa from an initial pressure of 13.3 MPa. For this solution the binodal is 12.9 MPa. The imposed quench takes the system to about 1.5 MPa below the binodal. For this quench the system undergoes spinodal decomposition. A series of similar experiments with different pressure quench depths were conducted at this concentration to determine the gap of the metastable region. The crossover from nucleation and growth to spinodal decompositon was determined to take place at 11.8 MPa. Since the binodal is 12.9 MPa, for pressure quenches within 1.1 MPa from the binodal point, the system enters the metastable region, and phase separation proceeds by the nucleation and growth mechanism. If the penetration is deeper than 1.1 MPa from the binodal point, the system enters the unstable region, and the phase separation proceeds by spinodal decomposition.

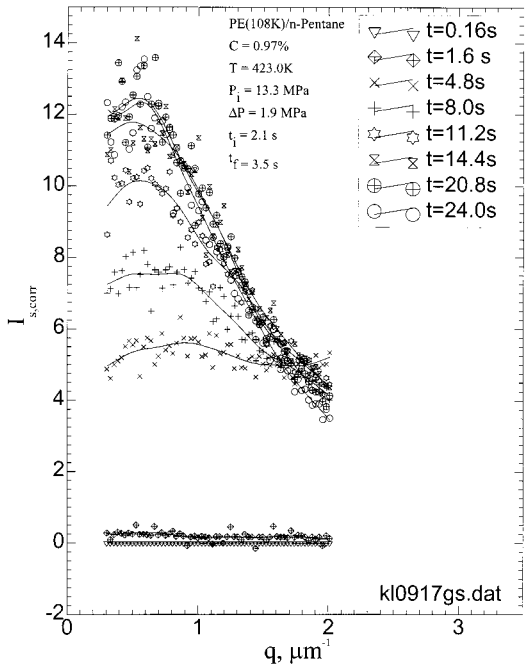

Figure 7. Evolution of the scattered light intensities with time as a function of the wavenumber q after a pressure quench of $\Delta P = 1.9$ MPa in 0.97% by mass solution of PE (108K) in *n*-pentane at 423.0 K. The total observation time is 24.0 s.

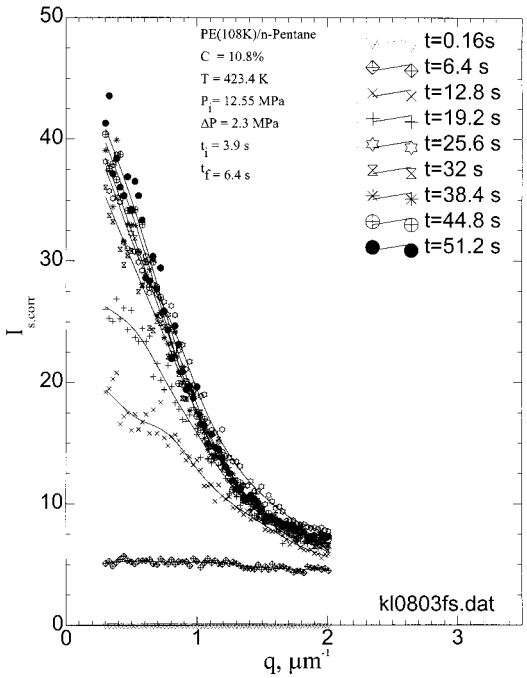

Figure 8. Evolution of the scattered light intensities with time as a function of the wavenumber q after a pressure quench of $\Delta P = 2.3$ MPa in 10.8% by mass solution of PE (108K) in *n*-pentane at 423.4 K. The total observation time is 51.2 s.

Figure 8 shows the scattered light intensity profiles during phase separation for the 10.8% solution. Here the scattered light intensities increase with time at all angles with an angular variation that is characterized by a continual increase in the scattered light intensity with decreasing q values. The spinodal ring could not be observed for shallow or deep quenches. The metastable gap at this concentration therefore must be very large.

From the experiments conducted at a range of concentrations for this system, the pressure corresponding to crossover from nucleation and growth to spinodal decomposition mechanism has been determined and identified as the spinodal pressure. These results have also been included in Table 1. Figure 9 is a pressure−concentration ($P-X$) diagram that includes the binodal pressure and the crossover pressures from nucleation and growth to spinodal decomposition. The shape of the binodal in Figure 9 is not arbitrary. Extensive prior work[12] showed the flat nature of this curve up to high concentration. As shown in this figure, the metastable gap becomes very narrow at about 2.0%, which can be taken as the critical polymer concentration for this polymer−solvent system. It should be noted that for this system the spinodal and binodal curves appear to merge at the maximum of the binodal curve. This is different from the poly(dimethylsiloxane) + CO_2 system[18] where a broad molecular weight distribution PDMS (PDI = 2.99) sample has been used; the binodal and spinodal were found to merge at a concentration higher than that corresponding to the maximum of binodal. In monodisperse systems, the binodal and the spinodal boundaries are expected to merge at the apex of the binodal. In the present system, the polydisperity of the polymer is 1.32, which is relatively narrow, and thus the merge at the apex is as anticipated. For a broader molecular weight distribution PE sample (PDI = 4.3), the location indeed

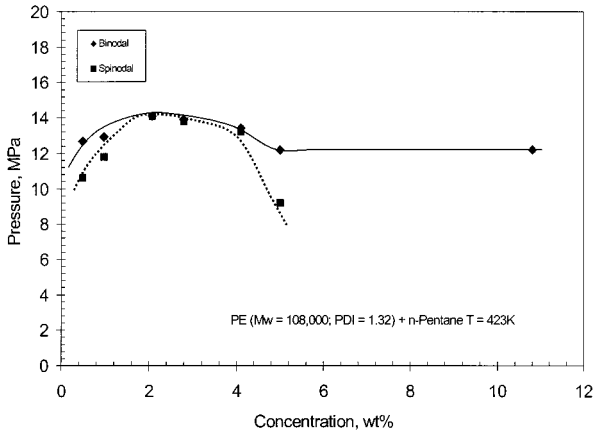

Figure 9. Pressure−composition phase diagram and the experimentally determined spinodal and binodal envelopes for PE (108K) + *n*-pentane system at temperature 423 K.

shifts to higher concentration,[24] which will be reported in a future publication.

Further Analysis of the Time Evolution of the Scattered Light Intensity during Spinodal Decomposition

Early Stage. The early stage of spinodal decomposition is often analyzed according to the Cahn−Hilliard theory.[6,15,16,19] This theory suggests that the scattered light intensities should show an exponential growth with time in the early stage of spinodal decomposition according to

$$I(q,t) = I(q,0)\exp(2R(q)t) \qquad (3)$$

Here q is the wavenumber of growing fluctuations, and $R(q)$ is the rate of growth of concentration fluctuations given by

$$q = \frac{4\pi}{\lambda}\sin(\theta/2) \tag{4}$$

$$R(q) = D_{app}q^2\left[1 - \frac{q^2}{2q_m^2}\right] \tag{5}$$

where λ is the wavelength and θ is scattering angle. D_{app} is the apparent diffusivity, and q_m is the wavenumber corresponding to maximum growth rate of fluctuations. The apparent diffusivity can be calculated from plots of $R(q)/q^2$ as the limiting value of $R(q)/q^2$ as q approach to 0, that is

$$D_{app} = \lim_{q\to 0}\{R(q)/q^2\} \tag{6}$$

Figure 10 shows the variation of the logarithm of scattered light intensity at selected angles with time for 2.07% solution subjected to 0.44 MPa quench at 423 K corresponding to data shown in Figure 5. It should be noted that from Figure 5 the pressure quench in this experiment was initiated at $t = 2.8$ s and ended at $t = 3.9$ s. Figure 5 and other quench data discussed in the previous sections showed that the location of the scattered light intensities is not stationary in time and moving to lower angles. This is in contrast to what would be the case if the system were in the early stage of spinodal decomposition. In the Cahn−Hilliard theory, in the early stage, the light intensity maximum I_m (q_m, $t \approx 0$) is observed at a time-invariant q_m. The early stage for the present system must therefore either have taken place in the time interval before 3.5 s or occurred at higher q value than accessible in the present system. Indeed, a recent publication that has focused on the very early stage of spinodal decomposition in polypropylene + trichlorofluoromethane suggests that the stationary q_m is possibly observed at times below 100 ms and at about $q \approx 2.8\ \mu m^{-1}$.[15]

With the present data sets, Figure 10 suggests that an exponential growth region can still be identified at short times. The Cahn−Hilliard analysis, if applicable, can be tested in this early stage of phase separation. From the slope of the linear region in this early part of the phase separation, the growth rates $R(q)$ at each q have been calculated. The variation of $R(q)/q^2$ vs q^2 is shown in Figures 11 for the pressure quench depth of 0.54 MPa. In the figure, the data have been extrapolated to $q = 0$ using only the high q values so that the q_m value would better represent the corresponding value that would be applicable in the true early stage of phase separation. An apparent diffusion coefficient of 9.5×10^{-12} m^2/s is indicated for this quench. Similar experiments conducted for quenches of 0.25 and 0.44 MPa led to diffusion coefficient of 1.4×10^{-12} and 3.6×10^{-12} m^2/s. These data show that D_{app} depends on the quench depth. The deeper the pressure quench, the larger is the diffusion coefficient, and the faster is the phase separation process. These values of diffusion coefficient are somewhat higher than the value we obtained in the poly(dimethylsiloxane) + CO_2 system in which the values of D_{app} were in the range from 0.5×10^{-12} to 2.5×10^{-12} m^2/s.[18] One reason for this is the higher temperatures (423 K) involved with the present system. For the polypropylene + trichlorofluoromethane at 452 K, D_{app} values that have been estimated are in the range of $(1.5-4.0) \times 10^{-12}$ m^2/s, which are very similar to the PE values obtained in the present study.[15] The data on the polypropylene system also show that the apparent diffusion coefficient becomes large for deeper quench experiment as observed in the present study.

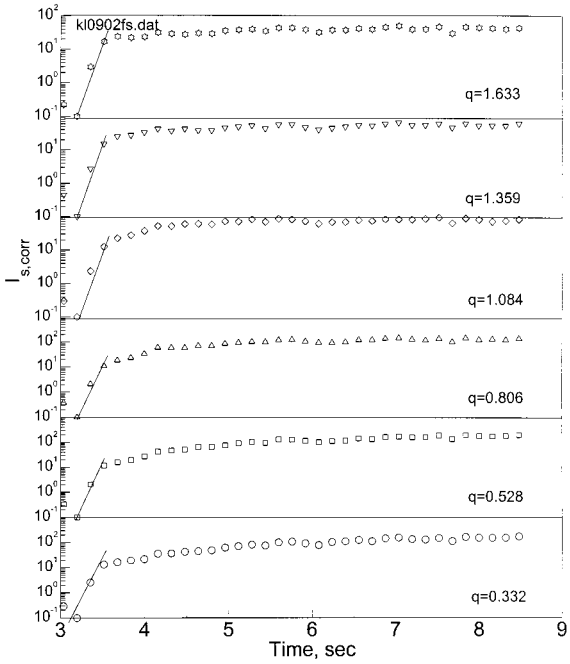

Figure 10. Logarithmic plot of the variation of the scattered light intensity as a function of time at selected wavenumbers during the early stage of phase separation. The slopes of the linear region provide information on $R(q)$, the rate of growth of concentration fluctuations.

Intermediate and Late Stage. The intermediate and late stage of spinodal decomposition[13,23,25,26] are often described in terms of power-law relationships of the type

$$I_m(t) \sim t^{\beta} \tag{7}$$

$$q_m(t) \sim t^{-\alpha} \tag{8}$$

These relationships provide a scaling description in terms of the exponents β and α of the time evolution of the scattered light intensity maximum I_m and the corresponding wavenumber q_m.

Figure 12 shows the variation of $\log(q_m)$ and $\log(I_m)$ with $\log(t)$ for the 0.44 MPa quench experiment. From this figure, the exponents are determined as $\alpha = 1.09$ and $\beta = 2.15$. The analysis of the data for quench depth of 0.54 MPa resulted in the exponent values of $\alpha = 1.24$ and $\beta = 2.47$.[24] These results show that the exponents obey a relationship $\beta \approx 2\alpha$, which is similar to the results reported for poly(dimethylsiloxane) + CO_2 and polystyrene + methylcyclohexane systems[18,19] undergoing pressure-induced phase separation. The values of α and β depend on the quench depth. They are larger when the pressure quench is deeper, which means that the development of the microstructure proceeds more rapidly.

Domain Size Growth. The maximum value of the wavenumber q_m is related to the dominant size scale, which is expressed as[23]

$$L = 2\pi/q_m \tag{9}$$

Time evolution of domain size can then be determined from time-dependent variation of q_m which is shown in

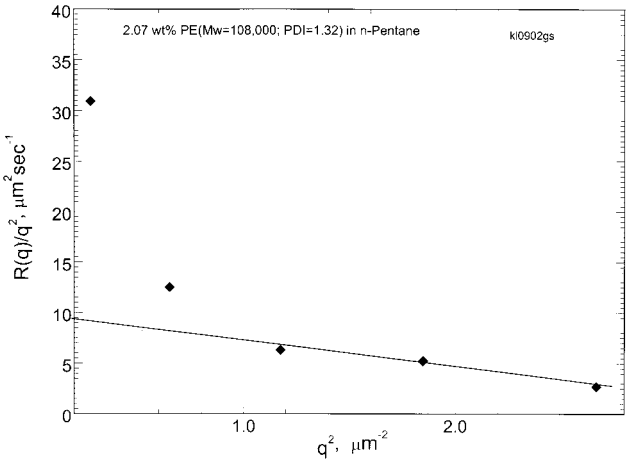

Figure 11. Determination of apparent diffusivity by extrapolation of the $R(q)/q^2$ data from high q values in 2.07% PE (108K) in *n*-pentane solution; quench depth $\Delta P = 0.54$ MPa.

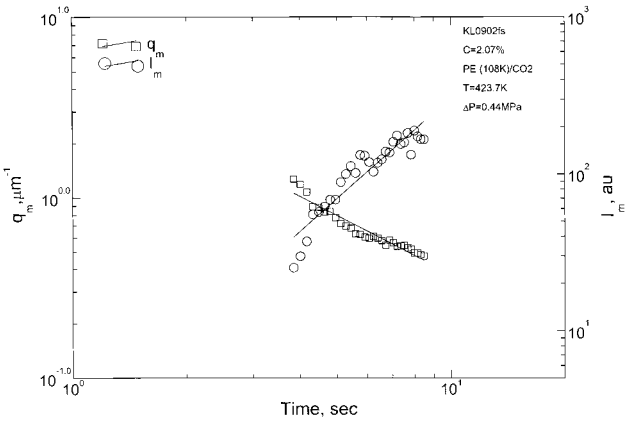

Figure 12. Power-law dependence of q_m and I_m on time.

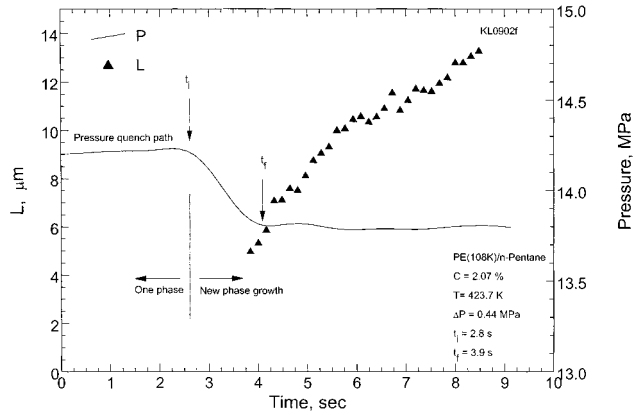

Figure 13. Evolution of the domain size with time. The actual time corresponding to the beginning and the end of the quench are indicated as t_i and t_f in the figure inset.

Figure 13. In this figure, the pressure quench path indicates the initiation of pressure quench, t_i, and the time corresponding to the end of the pressure quench, t_f. From the figure it is clear that the spinodal ring as reflected by the observation of scattered light intensity maximum at q_m is detected even before the pressure reaches its minimum. The domain size continues to increase with time from about 4 to 14 μm within 5 s.

Dynamic Similarity of Phase Growth. For systems that display dynamic similarity, Furukawa[27] has developed scaling functions in the form of

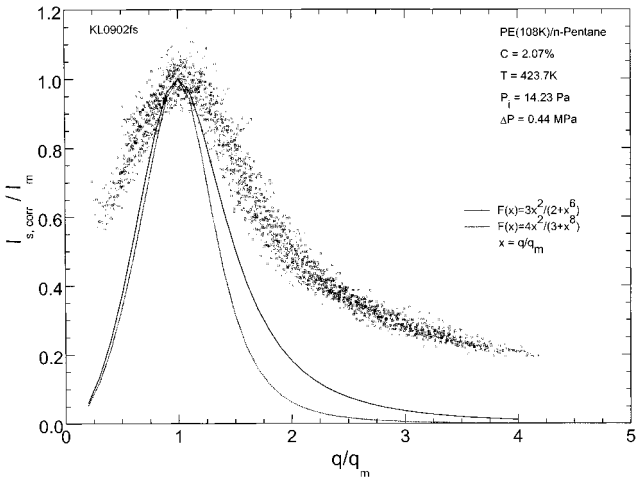

Figure 14. Test of the dynamic scaling hypothesis for the reduced structure factor. The data correspond to 2.07% solution subjected to 0.44 MPa pressure quench as shown in Figure 5. The different time data scale and collapse toward a master curve. The solid and dotted curves are the predictions from the Furukawa universal scaling functions for off-critical and critical quenches, respectively.

$$F(x) = 4x^2/(3 + x^8) \quad \text{(critical quench)} \qquad (10)$$

$$F(x) = 3x^2/(2 + x^6) \quad \text{(off-critical quench)} \qquad (11)$$

where $x = q/q_m$.

In such a system, the plot of $F(x)$ vs x ($x = q/q_m$) should collapse to a single curve for all times. Figure 14 is such a plot for 2.07% solution at 423.7 K for a 0.44 MPa quench. This corresponds to the time evolution data shown in Figure 5. At this concentration, the reduced data points indeed collapse to a single master curve, which may be a suggestion of self-similarity. However, the experimental data do not obey the theoretical Furukawa scaling functions for the critical or off-critical quenches. The theoretical curves are also included in Figure 14. The experimental data deviate more from the theoretical Furukawa scaling expectations as q moves away from q_m.

Conclusions

Pressure-induced phase separation in polymer solutions is a fast process. Controlled pressure quenches into the region of immiscibility while monitoring the time evolution of the angular variation of scattered light intensities permits determination of the experimentally accessible spinodal boundary. It is shown that, at or near the polymer critical concentration, the spinodal regime is experimentally accessible for both shallow and deep quenches. At concentrations further removed from the critical point, the metastable gap becomes large and spinodals are difficult to reach. Kinetics of spinodal decomposition in the intermediate and late stage are well described by power-law model, and the domain growth displays elements of self-similarity. Early time data permit estimation of the diffusion coefficient according to Cahn−Hilliard theory.

Acknowledgment. The experimental part of this work was completed while the authors were at University of Maine. The laboratory has been moved, and this research is now continued at Virginia Tech.

References and Notes

(1) Kiran, E. Polymer formation, modification and processing in or with supercritical fluids. In *Supercritical Fluids: Fundamentals for Application*; Kiran, E., Levelt Sengers, J. M. H., Eds.; Kluwer: Dordrecht, 1994; pp 541−588.
(2) Nishi, T.; Wang, T. T.; Kwei, T. K. *Macromolecules* **1975**, *8*, 227.
(3) Hashimoto, T.; Kumaki, J.; Kawai, H. *Macromolecules* **1983**, *16*, 641.
(4) Kyu, T.; Saldanha, J. M. *Macromolecules* **1988**, *21*, 1021.
(5) Snyder, H. L.; Meakin, P. *J. Chem. Phys.* **1983**, *79*, 5588.
(6) Izumitani, T.; Takenaka, M.; Hashimoto, T. *J. Chem. Phys.* **1990**, *92*, 3213.
(7) Bates, F. S.; Wiltzius, P. *J. Chem. Phys.* **1989**, *91*, 3258.
(8) Langer, J. S. *Phys. Rev. A* **1975**, *11*, 1975.
(9) Tao, J.; Okada, M.; Nose, T. *Polymer* **1995**, *36*, 3909.
(10) Kim, B. S.; Chiba, T.; Inoue, T. *Polymer* **1995**, *36*, 43.
(11) Hashimoto, T. *Phase Transition* **1988**, *12*, 47.
(12) Zhuang, W.; Kiran, E. *Polymer* **1998**, *39*, 2903.
(13) Lal, J.; Bansil, R. *Macromolecules* **1991**, *24*, 290.
(14) Steihoff, B.; Rullmann, M.; Kuhne, L.; Alig, I. *J. Chem. Phys.* **1997**, *107*, 5217.
(15) Kojima, J.; Takenaka, M.; Nakayama, Y.; Hashimoto, T. *Macromolecules* **1999**, *32*, 1809.
(16) Kiran, E.; Zhuang, W. *J. Supercrit. Fluids* **1994**, *7*, 1.
(17) Kiran, E. Polymerization and polymer modification in near- and supercritical fluids. In *Proceedings of the International Meeting on High-Pressure Chemical Engineering, March 3−7*; Karlsruhe, 1999; pp 3−12.
(18) Liu, K.; Kiran, E. *J. Supercrit. Fluids* **1999**, *16*, 59.
(19) Xiong, Y.; Kiran, E. *Polymer* **2000**, *41*, 3759.
(20) Xiong, Y.; Kiran, E. *Rev. Sci. Instrum.* **1998**, *69*, 1463.
(21) Hashimoto, T. Structure formation in polymer mixtures by spinodal decomposition. In *Current Topics in Polymer Science*; Ottenbrite, R. M., Utrachi, L. A., Eds.; Hanser: New York, 1987; Vol. II.
(22) Utracki, L. A. Thermodynamics and kinetics of phase separation. In *Interpenetrating Polymer Networks;* Klempner, D., Sperling, L. H., Eds.; Adv. Chem. Ser. Vol. 239; American Chemical Society: Washington, DC, 1994; pp 77−123.
(23) Hashimoto, T. Self-assembly of polymer blends at phase separation morphology control by pinning of domain growth. In *Progress in Pacific Polymer Science*; Imanishi, Y., Ed.; Springer: Berlin, 1992; Vol. 2, pp 175−187.
(24) Liu, K. M.S. Thesis, University of Maine, 1999.
(25) Takeno, H.; Hashimoto, T. *J. Chem. Phys.* **1998**, *108*, 1225.
(26) Utracki, L. A. Thermodynamics and kinetics of phase separation. In *Interpenetrating Polymer Networks;* Klempner, D., Sperling, L. H., Eds.; Adv. Chem. Ser. Vol. 239; American Chemical Society: Washington, DC, 1994; pp 77−123.
(27) Furukawa, H. *Physica A* **1984**, *123*, 497.
(28) Li, J.; Zhang, M.; Kiran, E. *Ind. Eng. Chem. Res.* **1999**, *38*, 4486.

MA000816K